

# Atmospheric Corrosion of Carbon Steel, Aluminum, Copper and Zinc in a Coastal Military Airport in Greece

Charalampos Titakis\*, Panayota Vassiliou and Ioannis Ziomas†

\* Corresponding author. E-mail address: [c.z.titakis@gmail.com](mailto:c.z.titakis@gmail.com), [ctitakis@central.ntua.gr](mailto:ctitakis@central.ntua.gr) (Major C. Titakis).

Laboratory of Physical Chemistry, School of Chemical Engineering National Technical University of Athens, 9 Heron Polytechniou, 15780, Athens, Greece

**Abstract.** The effects of relative humidity (RH), temperature (T), sulphur dioxide (SO<sub>2</sub>) concentration and chlorides deposition rate on the corrosion of Carbon Steel, Aluminum, Copper and Zinc at the rural and coastal environment of Pachi military airport, after 2 years of outdoor exposure, are presented. A classification of the corrosivity of the airport atmosphere was based both on environmental data and the corrosion rate measurements of carbon steel and aluminum standard specimens, after the first year of exposure, according to ISO standards and ASTM norms. A systematic investigation is carried out for the two-year outdoor exposure period for all the tested metals based on corrosion rates determination and corrosion products characterization. The findings underline the necessity of field studies results, in order to locally optimize the cost-benefit ratio in all steps of the aircrafts life-cycle.

**Keywords:** Atmospheric corrosion; corrosion management; military airport; corrosion damage algorithm

## INTRODUCTION

Atmospheric corrosion constitutes a major problem with regard to the deterioration of construction materials, especially metals. The importance of the phenomenon of corrosion, as a consequential factor in the protection of human constructions is firstly understood by the economic implications and also the intensity of the efforts being made locally and internationally to mitigate it. Several studies have concluded that corrosion costs at about 3-6% of the Gross Domestic Product of the industrialized nations, where atmospheric corrosion plays a main part [1-5]. Organized attempts to understand the phenomena of atmospheric corrosion and at the same time to develop prediction models of environmental corrosivity began in 1980, when three programs studying atmospheric corrosivity worldwide were initiated. With the participation of countries on four continents, Europe, America, Asia and Oceania, the ISOCORRAG, ICP/UNECE and MICAT programs were launched. Despite their differences there were a number of similarities of the basic methodologies. The main goals were to establish the Dose Response Functions (DRF) based on the acquired experimental data: meteorological (Temperature (T), Relative Humidity (RH), Precipitation (P), and Time Of Wetness (TOW)), pollution (SO<sub>2</sub> and NaCl) and the determination of a methodology in order to be used for the classification for the atmospheric corrosivity. As a result in 1992, the publication of ISO 9223-9226 [6-9] was a major step for the atmospheric severity methodology, evaluation and

classification from the viewpoint of outdoor exposure of metal specimens considering a relatively small spectrum of climatological and pollution conditions. Additionally, an extensive research has been carried out on the damage response functions and corrosion severity. In the work of Morcillo et al [10] the corrosion data obtained in the ISOCORRAG and MICAT programs analyzing the corrosivity categories are compared to those estimated on the basis of ISO standard 9223 [6] for the four reference metals. The correlation coefficients obtained for the damage functions of the 4 metals were hardly improved.

Many systematic research works that followed, suggest that the most significant changes, from the atmospheric corrosion point of view, was the decrease in the SO<sub>2</sub> pollutant concentration, the increase in other types of air pollution and the increase of the average annual precipitation and temperature over the course of the 20th century. Carbon steel corrosion rate has decreased exponentially at non-marine sites (urban, industrial and rural) and specifically by 50% about each 12-year period for industrial and urban sites and each 16-year period for rural sites [1], during the last decades, mostly due to the reduction of sulphur dioxide's emissions globally. A study of the atmospheric corrosion of the copper, zinc and aluminum exposed outdoors on a coastal, an urban-industrial and a rural environment for 18 months concluded that the interaction between the chloride deposition rate with the time of rainfall effects the corrosion of the three non-ferrous metals in the most dominant way [2]. A future dominant role of chloride deposition in atmospheric corrosion of metals in Europe's coastal and near-coastal areas is also expected [11].

There are other studies that record and evaluate the long-term trends of corrosion and the functional life of manufactured products. Pourbaix [12] and McCuen et al [13] suggest that a 4-year corrosion versus time function is required in order to estimate the 20-30 year corrosion behavior of metals in a certain atmosphere, or 10 years in order to predict the infrastructures or the manufactured products life-cycle. Summitt and Fink in 1980 [14] developed the Corrosion Damage Algorithm (CDA) for the United States Air Force (USAF). The CDA considers first the distance to the salinity factor (sea salt water) leading either to the very severe (AA) grade or judging by the moisture parameters. The CDA was recommended to USAF, by NATO Research and Technology Organization (2011), as a basic tool in order to succeed an initial estimation of the classification of atmospheric severity and as a guide to maintenance and logistic decisions [15]. The last call to set the appropriate maintenance intervals remains in the capability and the experience of the local management, based on the field measured meteorological and pollutant parameters and of the atmospheric corrosivity [14,15]. The models usually employed in order to predict the corrosion damage are statistical regression models, which have been demonstrated as being locally accurate [16,17], but limited when the available environmental and corrosion data are characterized as highly non-linear [18-20]. Artificial Neural Network (ANN) method for metals is also used for modeling non-linear multi-parametric systems [18,19] usually employing the data from (i) the literature of long term exposure tests of metals and (ii) at least five atmospheric corrosion stations. Jianping et al [21] employing the data from literature for long term exposure tests presented an ANN modeling which is, under certain conditions, successful and is not as trustworthy for very long term data. Their results are also better, than those of Feliu et al [18,19,21]. No significant results were obtained by the described artificial neural network models using data collected from less than five atmospheric corrosion stations, after a research in the relevant literature. The ANN can be designed and trained to estimate corrosion rates of metals using meteorological and pollutants data, the exposure time as the input and the experimental metal loss as the output vector, with a relatively small error. An ANN model

designed and trained in order to predict steel corrosion loss after long-term exposure in the Czech Republic calculated the models error at 6% [22]. Despite the fact that all the earlier methodologies (ISOCORRAG, ICP/UNECE and MICAT programs, ISO methodology etc.) have some limitations and new atmospheric corrosion models, which take into consideration the nonlinearity of the accelerating effect of meteorological and pollution variables instead of the mean values of these factors are proposed [23], the ISO standards [6-9] are still regarded as the only reliable and globally accepted methodology to assess the corrosivity by measuring the corrosion rates of standard metal samples and defining the corrosivity category of the atmosphere [24].

In order to succeed a more accurate regional corrosion mapping with high correlation coefficient -which is the main aim of all the relevant programs and researches- and to assess the severity of complex corrosion environments such as coastal industrial establishments, airports, military infrastructure, new approaches in atmospheric corrosion modeling should emerge. The results of site-specific case studies could contribute in existing models improvement or could be utilized in new algorithms training. East Mediterranean countries, such as Greece, have poorly or not at all participated in this global effort. Greece has around 2,800 islands [25] and 13,676 kilometers of coastline [26]. Additionally, the proximity to the sea at the major part of its continental region is a strong indication for relatively high chlorides deposition rate, also, as well as inland. In Greece, an extensive corrosion damage of metal based constructions has been observed. These costs are present in all steps of every infrastructure or product life-cycle, from material selection, design and installation to maintenance intervals and repair.

The present work stems from the need to effectively reduce the corrosion-related damage costs of military aircrafts helicopters and infrastructure. It also aims to optimize the maintenance management and to increase service life of the aircrafts. In order to optimize the corrosion management and select the appropriate protection method a proper understanding of the local corroding system is required. Therefore, commercially pure aluminum, unalloyed carbon steel, zinc and copper have been employed for a long-term atmospheric corrosion study, according to ISO and ASTM norms [6-9,27-31] and a literature review on relevant sources was undertaken [32-39], in the rural and coastal site of a military airport in an effort to assess corrosion impact on aviation installations near the seashore. A classification of the corrosivity of the airport atmosphere was performed both on environmental data and the corrosion rate measurements of carbon steel and aluminum standard specimens, after the first year of exposure, according to these ISO standards and ASTM norms. A systematic investigation -for all tested metals- is also carried out for a two-year outdoor exposure period, based on corrosion rates determination and corrosion products characterization. This approach did not use sensitive information or confidential data.

## **REGIONAL ENVIRONMENTAL PARAMETERS**

### **Meteorological Data**

The mean monthly rainfall, mean monthly wind speed and the prevailing wind at Elefsina and Pachi areas were analytically investigated and presented in [40] with the data that had been provided by the National Observatory of Athens (Megara station), the Ministry of Environment and Energy and the Hellenic Meteorological Service (station of Elefsina) [41-43]. In brief: The

wettest month (with highest rainfall) is December. The driest months (with lowest rainfall) are July and August. The mean annual rainfall amount of the area, during the period 1958-97, has been estimated around 37.29 cm. The mean annual wind speed of the area, during the period 2009-11, has been estimated at approximately 11.22 km/h (3.17 m/s), marginally greater than the threshold value of 11 km/h which is the “minimum wind speed (MWS) or threshold required for the entrainment of marine aerosols over a salt-water body” [34]. The monthly prevailing wind at Megara Area is presented at the Table below:

**TABLE 1.** Monthly prevailing wind at Megara Area (period: 1975 – 1991) [40,43]

Month	Prevailing Wind	Month	Prevailing Wind
JAN	NORTHWEST (NW)	JUL	NORTHWEST (NW)
FEB	NORTHWEST (NW)	AUG	NORTHWEST (NW)
MAR	NORTHWEST (NW)	SEP	NORTHWEST (NW)
APR	NORTHWEST (NW)	OCT	NORTHWEST (NW)
MAY	NORTHWEST (NW)	NOV	NORTHWEST (NW)
JUN	NORTHWEST (NW)	DEC	NORTHWEST (NW)
CALM: 31%			

## Pollutants

By taking into consideration the yearly evolution of the mean concentration values of gas pollutants over the Attica region for the decade 2000–2009, there is an almost constant presence of O<sub>3</sub>, with a mean concentration of 55 µg m<sup>-3</sup> [44]. In the industrial area of Elefsina, where the country’s industrial core is sited and in a distance of 20 km from Pachi airport, the annual mean concentration of SO<sub>2</sub> is at about 7 µg/m<sup>3</sup> [40,45,46].

No pollutant measurements have ever been made in the airport area. The concentration of sulfur dioxide at the airport is estimated, according to the European Monitoring and Evaluation Programme (EMEP) [47] and several sources [40,45-52]. Regarding the existence of pollutant SO<sub>2</sub>, namely the airport’s area has been studied and the annual maximum concentration of the pollutant estimated at [SO<sub>2</sub>]<sub>max</sub> = 2µg/m<sup>3</sup> [40,48].

## EXPERIMENTAL PROCEDURE

### Materials

Aluminum, zinc, copper and unalloyed carbon steel specimens have been exposed in outdoor atmospheric conditions, at the roof of a maintenance hangar, at a distance of approximately 0.2 km from the seashore at Pachi military airport respectively for a two-year exposure period. Exposure started in 2014 at two different periods of the year, in summer and in winter, in order to determine the seasonal effects on the initial corrosion stage and eventually the long term effects on the metal surface as well as the evolved corrosion rates. The standard specimens of commercially pure aluminum (>99.5%min), unalloyed carbon steel, zinc and copper are flat specimens of size 100 mm×100 mm×1 mm of current fabrication, as described in ISO 9226 [9]. Table 2 shows the detailed composition of the tested carbon steel samples as analyzed by an ARL3460 automatic Optical Emission Spectrometer (OES) at Halyvourgiki Inc. laboratories.

**TABLE 2.** Average chemical composition (wt.%) of unalloyed carbon steel specimens

Fe	C	Mn	S	P	Si	Ni	Cr	Cu	V	Al	Sn	Mo	Co	As	Ca	Nb	N	O	Pb
99.44	0.07	0.32	0.03	0.0069	0.007	0.02	0.02	0.04	0.0007	0.01	0.004	0.003	0.003	0.0017	0.0006	0.001	0.004	0.016	0.0008

### Selection of Exposure Site

The military airport of Pachi, Megara, Greece was selected as exposure site due to (i) the macroscopic observation of the corrosion in aircraft subassemblies and of the construction materials in helicopters, after technical inspection, (ii) the high costs in all steps of the aircrafts life-cycles worldwide and (iii) to the proximity of the rural test site to the seacoast and to the surrounding industrial area of Elefsina.

### Preparation of the Specimens and of the Installation at the Exposure Site

Four test pieces were used for each metal and period of exposure on a rack at 45° to the horizontal facing south, as seen in Figures 1 and 2. The metal structures were designed with the use of “3D CAD Design Software SOLIDWORKS”, according to standard ISO 9225 [8], and constructed in the Laboratory of the Manufacturing Technology of NTUA. Three specimens, for each metal and period of exposure, were weighted before and after the exposure in order to measure the weight loss. The preparation, cleaning of the metal coupons (and the mass loss of the exposed metal samples was determined after sequential pickling as per ISO 8407 [28] and the ASTM norm, G1-90 [29]. Chemical cleaning procedures for the removal of the corrosion products are described in Table 3.

**TABLE 3.** Chemical cleaning procedures for removal of corrosion products after the exposure

Metal	Chemical	Time	Temperature
Aluminum	50 ml phosphoric acid, 30 gr chromium trioxide, distilled water to make 1lt.	10 min	80°C to boiling
Steel	250 ml hydrochloric acid with inhibitor, distilled water to make 1000 ml.	10 min	20-25°C
Zinc	150 ml ammonium hydroxide, distilled water to make 1000 ml.	5 min	20-25°C
Copper	500 ml hydrochloric acid, distilled water to make 1000 ml.	3 min	20-25°C



**FIGURE 1.** Outdoor exposure of the flat metal specimens at the airport. On the frame, the Tinytag PLUS 2 data logger with Temperature/Relative humidity probe



**FIGURE 2.** Device used for “Determining Atmospheric Chloride Deposition Rate by Wet Candle Method” at the airport. Facing the sea in a distance of 150 m from the seacoast

### Corrosion Evaluation Methodology

Three test specimens for each metal and period of exposure were used for gravimetric analysis. The fourth test specimen for each metal was used for the analysis of the corrosion products formed on the metal surface. All samples were weighed before and after exposure. Test work was carried over 2 years, with samples taken for analysis after 3, 6, 12 and 24 months during the two periods of exposure. “TableCurve 2D v5.01.01” and “Microsoft Excel” programs were used for the determination of the power equations and for plotting the data relative to the corrosion loss. Corrosion rates were determined from the weight loss of specimens in accordance

with ISO 9226 [9]. The obtained data were used for the classification of atmospheric corrosivity according to ISO 9223 [6]. The corrosion products formed on the metal surfaces have been characterized by: (i) The FEI Quanta 200 Scanning Electron Microscope/Energy Dispersive Spectrometer (SEM/EDS) coupled with Energy Dispersive X-Ray Analysis (EDAX). The SEM images were analyzed by means of the computer program EDGE.EXE [53]. (ii) The Siemens D-500 X-ray diffractometer (with a graphite crystal monochromator and a Cu anticathode) based on an automatic adjustment and analysis system, with Diffract-EVA quality analysis software [54]. (iii) A Leica DMR Optical Microscope (OM). (iv) The aluminum surface morphology examination was by an Atomic Force Microscope Scanner (AFM) DUALSCOPE 95-50 of DME.

Carbon steel and aluminum specimens are also exposed each year since 2014 for a 1-year exposure period, during winter (the worst case scenario as concerns the direct corrosion of the 2 metals at Pachi Airport region), in order to examine the reliability of the Corrosion Damage Algorithm at the airport's region.

### **Recording of T and RH at the Test Site**

The parameters of air temperature ( $T$  °C) and of relative humidity (RH%) were obtained by a temperature and RH data logger «Tinytag» PLUS2 (TGP-4500) for a year at the exact field sites, as seen in the frame of Figure 1. T and RH were also used for calculating the Time of Wetness (TOW) using the procedure given in ISO 9223 [6].

### **Airborne Salinity Determination**

Airborne salinity by chloride is in the process to be measured by the Wet Candle Method for the airport according to ISO 9225 [8] and ASTM G140-02 [27] standards. Sampling is performed every 30 days, while a new sample is positioned for further exposure. The amount of chlorides, in every sample, is measured by both the Mohr and Volhard titration methods, as well as by  $\text{AgNO}_3$  test.

## **RESULTS AND DISCUSSION**

### **In-situ Measurement of Airport's Meteorological Conditions**

The monthly variation of the temperature-humidity data and the time of wetness are presented on Figure 3.

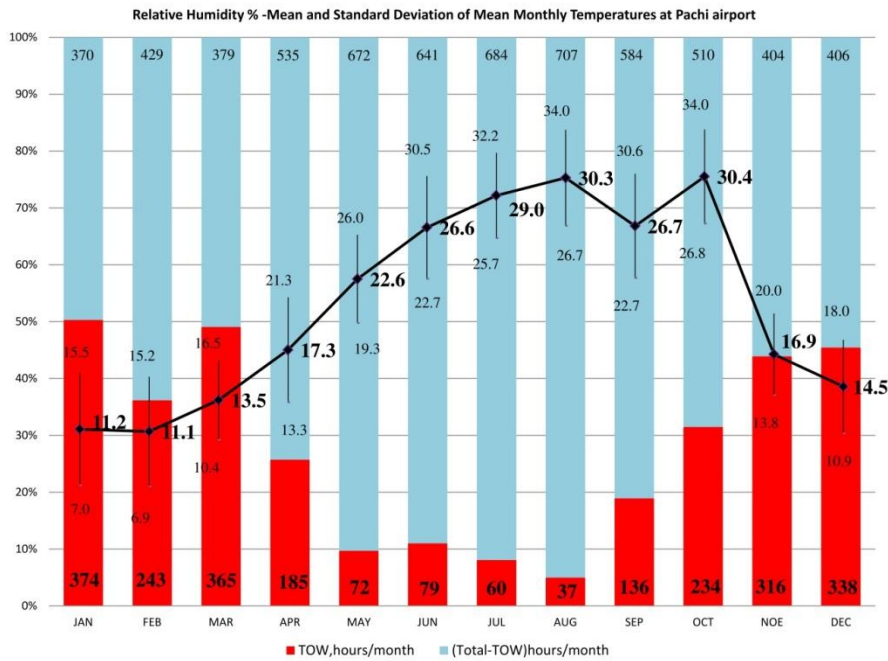


FIGURE3. Monthly variation of T (°C) and RH (%) data at the Airport Area

The Time of Wetness expressed in hours per year is estimated in 2,439 hours/a. The RH-TOW factor is expected to affect the atmospheric corrosion of metals in a major degree. The influence of temperature on the atmospheric corrosion of many metals has a maximum at about 9-11 °C. The mean annual temperature at the airport is 20.9°C. According to a previous study [40], the concentration of sulphur-containing substances represented by SO<sub>2</sub> is smaller than 12 µg/m<sup>3</sup>. Due to the NW prevailing wind at Megara area, from inland to the seashore and the mean annual wind speed [40] the salinity is expected to affect the corrosion of metals to a lesser degree than what is generally expected for a coastal site.

### The 2-Year Corrosion Evolution of the Tested Metals and Classification of the Corrosivity of Pachi Airport Atmosphere

#### The 2-Year Corrosion Evolution of the Tested Metals

For modeling the data relative to the corrosion loss, the (power) kinetic equation (1) in the form:

$$y = a \times t^b \tag{1}$$

where a: a constant, t: time of exposure in days; and b: time exponent. The validity of the equation and its reliability to predict long-term corrosion has been demonstrated by many authors [19,55-62].

The constant “a” represents the corrosion loss during the first year, while the time exponent “b” represents the multi-year loss yield [63]. The lower the time exponent “b” term the more protective the corrosion product layer on the metal surface [64]. Both a and b constants are dependent on the type of metal and on the climatic parameters. The statistical correlation coefficient, R, is a measure of the grade of fit of the environment regression, and R<sup>2</sup>, the

coefficient of determination, expresses the fraction of total variance of the data explained by the regression [63]. Regression analyses of the time exponent “b” and “a” values against the environmental factors of TOW, sulfation and salinity, by SW Dean and DB Reiser [63], indicated that for all four metals, the time exponent regressions were barely or not at all significant with environmental variables and on the other hand, the “a” regressions were very significant in most cases.

The representation of the corrosion data versus time in a power plot are depicted at Table 4 and Figures 4-7 for each one of the tested metals. Figures 4-7 show the experimental gravimetric curves, when exposure starts during winter (upper curve) and during summer (lower curve), and the fitted model equations obtained for carbon steel, aluminum, copper and zinc metal specimens for the coastal site of Pachi for the two initial time of exposure (initial corrosion stage). Table 4 shows the mass loss data for 1 and 2 years determined experimentally and the model equation parameters and the estimation of 4-year corrosion by the projection of the model equations.

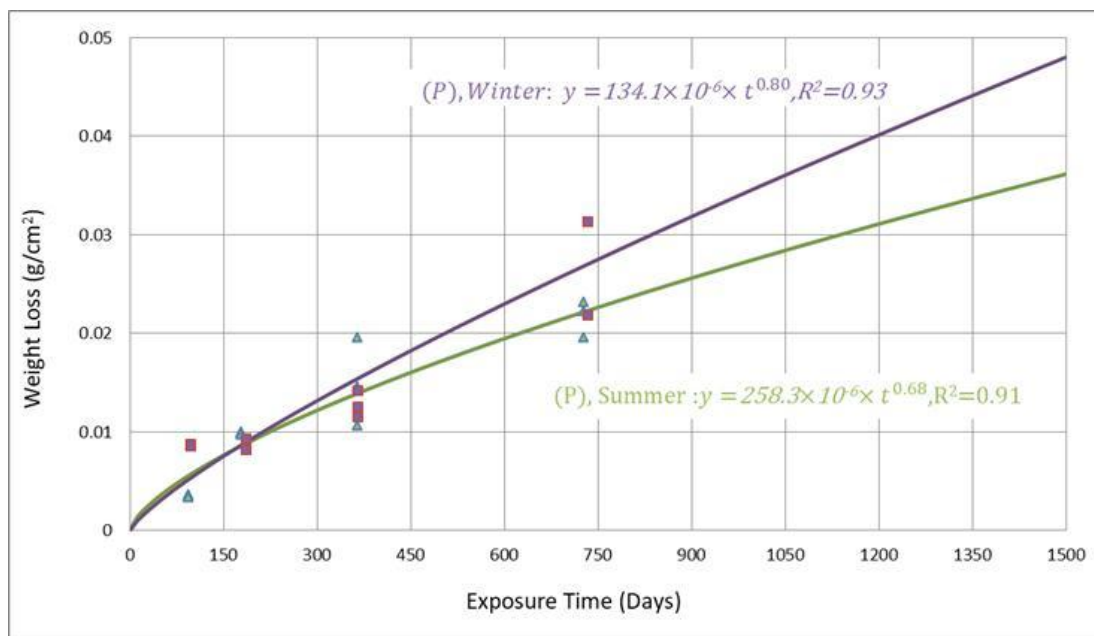


**FIGURE 4.** Experimental gravimetric curves, with exposure starting during winter (upper curve) and summer (lower curve), for unalloyed carbon steel and the fitted model equations.

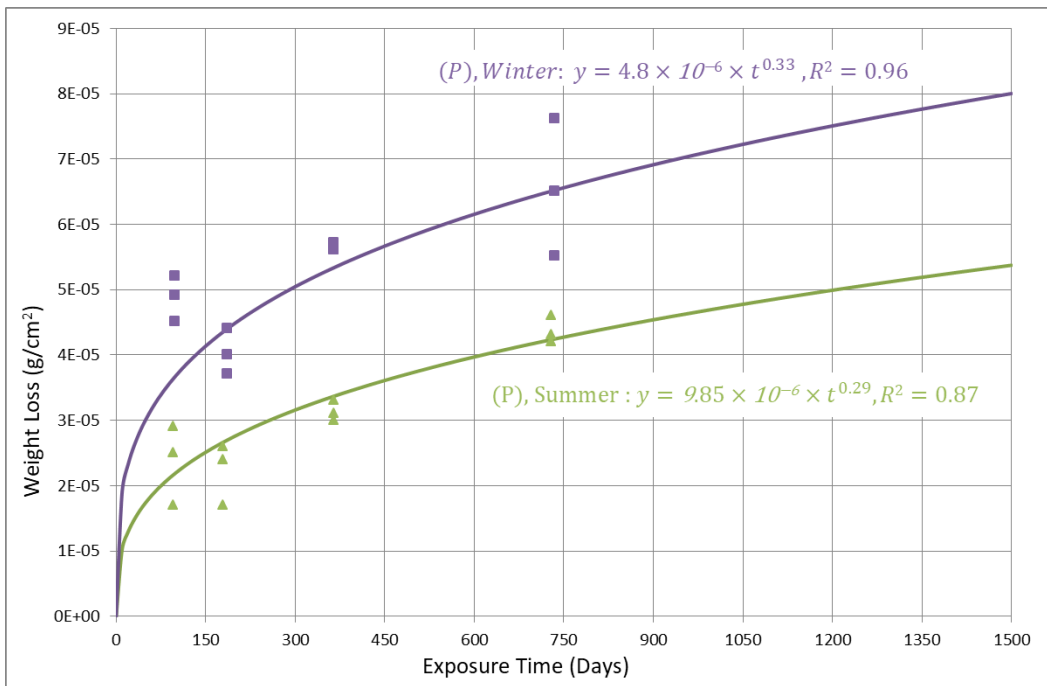


**FIGURE 5.** Experimental gravimetric curves, with exposure starting during winter (upper curve) and summer (lower curve), for Aluminum Alloy 1050 and the fitted model equations.

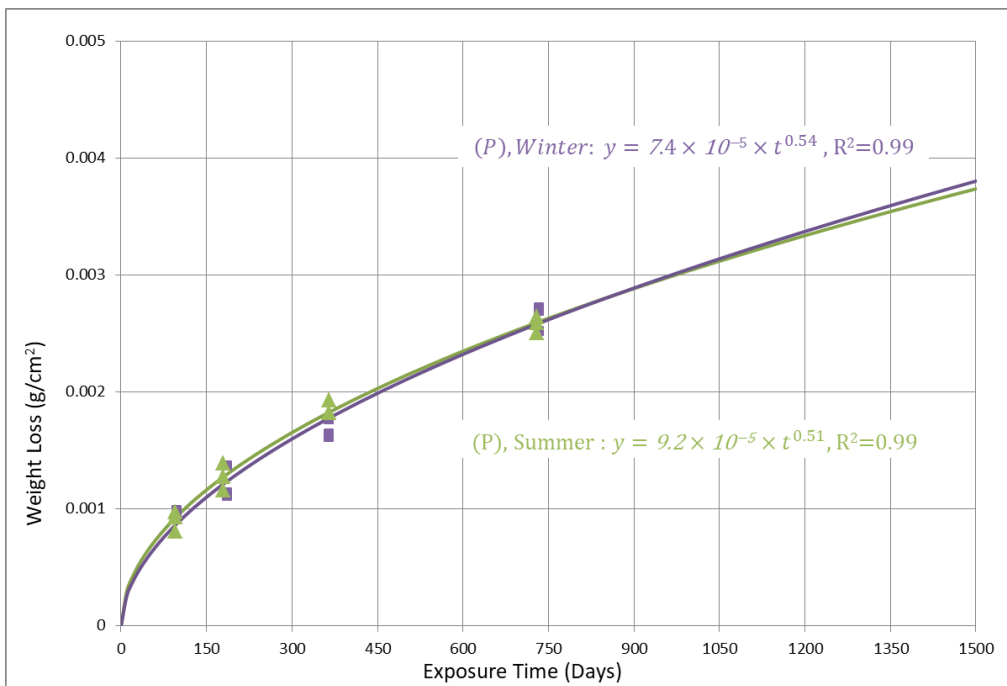


**FIGURE 6.** Experimental gravimetric curves, with exposure starting during winter (upper curve) and summer (lower curve), for Copper and the fitted model equations.

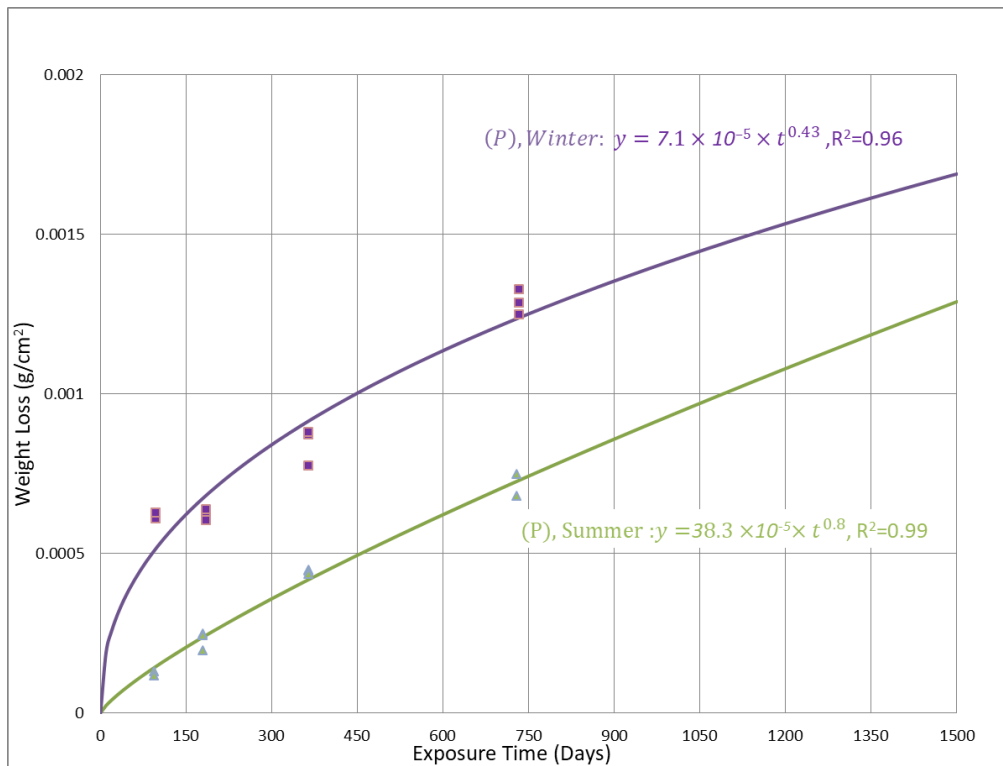


**FIGURE 7.** Experimental gravimetric curves, with exposure starting during winter (upper curve) and summer (lower curve), for Zinc and the fitted model equations

**TABLE 4.** Mass loss data for 1 and 2 years experimentally determined and the model kinetic parameters. Estimation of 4-year corrosion by the projection of the model equations

Metal	Exposure Start	Average Mass Loss (g/m <sup>2</sup> )			Calculated Kinetic Equations Constants		
		1 Year	2 Years	4 Years	a	b	R <sup>2</sup>
Carbon Steel	Summer	149.1	216.4	355	$258.3 \times 10^{-6}$	0.68	0.91
	Winter	126.5	281	470	$134.1 \times 10^{-6}$	0.80	0.93
Aluminum	Summer	0.31	0.44	0.53	$9.85 \times 10^{-6}$	0.29	0.87
	Winter	0.57	0.66	0.79	$4.8 \times 10^{-6}$	0.33	0.96
Copper	Summer	20.9	25.8	36.9	$9.2 \times 10^{-5}$	0.51	0.99
	Winter	16.7	26.4	37.5	$7.4 \times 10^{-5}$	0.54	0.99
Zinc	Summer	4.4	7.1	12.6	$38.3 \times 10^{-5}$	0.80	0.99
	Winter	8.4	12.9	16.7	$7.1 \times 10^{-5}$	0.43	0.96

In the case of carbon steel, the relatively small value of the time exponent agrees with the TOW observed at the airport environment. The value of the carbon steel time exponent in an atmosphere with higher TOW would be higher. Sulfation and salinity strongly affect the “a” constant [63]. The «a» values at the airport are relatively high due to the effect of sulphur-containing substances and salinity (due to the proximity to the sea). The “a” value is higher during summer at the airport probably due to the maximization of the frequency of aircraft technical tests and as a result the maximization of aircrafts fuel emissions (sulfation) in combination with the lower wind speeds which results to higher SO<sub>2</sub> and sea-salt deposition on the metal surfaces [63]. During the first year of exposure, steel exhibits an almost identical

corrosion rate and is independent of the period (summer or winter) initially exposed. Multi-year corrosion evolution shows that the synergistic effect of sea chlorides, from natural airborne salinity, with SO<sub>2</sub> plays a significant role in determining the corrosion rate of steel [65,66]. High RH-TOW, during the period December-March, and the decisive influence of temperature, during January and February increase the corrosion of steel specimens. Unalloyed carbon steel, exposed during winter, showed increased corrosion among the tested metals. The O<sub>3</sub> pollutant has little effect in steel corrosion rate and there is no synergistic effect of O<sub>3</sub> with the SO<sub>2</sub> pollutants [67].

In the case of aluminum, the “b” values are not strongly affected by environmental variations, due to the Al<sub>2</sub>O<sub>3</sub> spontaneous formation upon exposure in the environment, which protects the metal substrate. Sulfation and salinity affect the “a” value much less than the other three metals [41]. Aluminum exhibits the lowest “a” and time exponent “b” values than the other tested metals. The corrosion values found less than 0.30 g/m<sup>2</sup>a, during the multi-year corrosion evolution, are mainly the result of metal attack by the chemical reagent used during cleaning for gravimetric weight loss calculation rather than by the severity of the atmosphere [66]. The highest corrosion rate of aluminum specimens are observed at winter. That was expected mainly due to the effect of high RH-TOW, in relation to the samples exposed during summer, and secondarily due to the impact of salinity [58], because of the proximity to the sea. High RH-TOW, during the period December-March, and the mean monthly temperature, during January and February, also guide to the relatively increased corrosion attack. Aluminum corrosion rate is the lowest among the tested metals.

In the case of copper, salinity and TOW strongly affect both the time exponent and the “a” values. [63]. During the first year of exposure, copper corrosion rate is an order of magnitude lower than that of steel and independent of the initial period of exposure. Copper has a low corrosion rate because of its low thermodynamic tendency to react (low potential compared to iron). Copper also exhibits the highest coefficient of determination value (R<sup>2</sup>=0.99).

In the case of zinc, the environmental variables do not affect the protectiveness of the corrosion product to a great degree. TOW and chlorides affect the time exponent values to a small degree. Higher TOW reduces the protective capacity of corrosion layer. Sulfation strongly affects the “a” value, but not as strongly as steel [63]. When the zinc chloride is formed and there is no washing out by rain the layer does not increase, unless there is a continuous layer of electrolyte induced by the humidity which at night will form a water layer on the surface. From the first year of exposure, zinc exhibits corrosion rate dependent of the period initially exposed and an order of magnitude lower than steel, a fact that has been found by other researchers [68]. Higher RH-TOW play the catalytic role in corrosion rate of zinc [68]. The synergistic effect of the relative high moisture with sulphur dioxide [52] and relative high ozone concentration [69] in the atmosphere increases its corrosion rate. As it is observed, high concentration of SO<sub>2</sub> or high concentration of chlorides in the atmosphere leads to the dissolution of the protective corrosion layer and creates water-soluble corrosion products that lead to high corrosion rates of zinc [70-72]. Zinc corrosion rate decreases with time and that leads to the fact of relatively low concentration of both pollutants (SO<sub>2</sub> and chlorides), that confirms the results of this study and the classification analyzed below. In the marine atmosphere (P<sub>0</sub>) of the airport the corrosion of zinc is a direct function of TOW and the chloride pollution level [73]. The multi-year corrosion evolution shows that zinc specimens exposed during winter exhibit steadily higher corrosion rate, by at least 45%, than those exposed during summer.

Gravimetric data for the winter season: During the first 3 months of exposure higher weight loss values are obtained for aluminum, steel and zinc causing deviations from fitted

curves. This can be attributed to the water-solubility of the initial corrosion products. From the 6-month experimental data it is evident that both corrosion film dissolution and water-insoluble corrosion products accumulation take place.

### *Classification of the Corrosivity of the Pachi Airport Atmosphere*

Data on the corrosivity of the atmosphere are essential for the development and specification of optimized corrosion resistance for manufactured products. The corrosivity category is a technical characteristic which provides a basis for the selection of materials and consequently protective measures in atmospheric environments subject to the demands of the specific application particularly with regard to service life [9].

The airport atmosphere is classified by sulphur-containing substances represented by SO<sub>2</sub>, in accordance with ISO 9223 [6], in pollution category P<sub>0</sub> ([SO<sub>2</sub>] < 12 µg/m<sup>3</sup>), which is accounted to be background pollution by SO<sub>2</sub> and insignificant from the point of view of corrosion attack. The Time of Wetness expressed in hours per year is estimated in 2439 hours/a. As a result, the atmosphere is classified of TOW as «T3», according to ISO9223:1992 [6]. The characterization of an outdoor test site with respect to its corrosivity can be accomplished by determining the corrosion rate of standard specimens exposed for one year to the atmosphere at the respective location (direct corrosivity evaluation). The corrosion rate for the first year of exposure for the different corrosivity categories is presented at Table 5.

**TABLE 5.** Corrosion rates for the first year of exposure for the different corrosion categories according to ISO:9223 [6].

Corrosion Category	carbon steel (g/m <sup>2</sup> a)	Aluminum (g/m <sup>2</sup> a)
C1	≤10	Negligible
C2	11 – 00	≤0.6
C3	201 – 400	0.6 – 2
C4	401 – 650	2 – 5
C5	651 – 1500	5 – 10

The average chemical composition of commercially pure aluminium (>99.5% min) and of the unalloyed carbon steel (Cu 0.03% to 0.10%, P<0.007%) specimens used at this study meets the requirements described by ISO 9226. In contrast, zinc and copper, according to the commercial supplier, does not meet the requirements described by ISO 9226 [9]. As a result, the classification of the atmospheric corrosivity, for carbon steel and aluminum is presented at Table 6.

**TABLE 6.** First-year of exposure corrosion rate of carbon steel and aluminum and ISO classification of the atmosphere severity at the airport according to ISO:9223 [6].

Exposure Start	Metal (g/m <sup>2</sup> )	
	Carbon Steel	Aluminum
Pachi/Summer	149.1	0.31
Pachi/Winter	126.5	0.57
ISO Classification of Corrosivity of Atmospheres	C2 «LOW»	C2 «LOW»

The higher first-year corrosion rate of carbon steel specimens, exposed during summer, is primarily caused by the background pollution of the area (SO<sub>2</sub> and salinity) and the high conductivity of the steel specimens surface due to the existing Particulate Matters (PMs) in the area augmented by the North African dust (PM<sub>10</sub>) during the initial time of exposure.

According to the classification of the corrosivity of atmosphere, the airport atmosphere, with regard to pollution by airborne salinity, according to ISO 9223 [6], is expected to be classified as pollution category S<sub>0</sub> (deposition rate of chloride ≤ 3 mg/(m<sup>2</sup>d)) or S<sub>1</sub> (deposition rate of chloride in mg/m<sup>2</sup>d: 3<S<60). In relation with the corrosion products development and the atomic concentration of chloride observed on copper specimens (presented below), the chloride deposition rate is not insignificant, regarding the atmospheric corrosion, and it cannot be considered as background pollution. As a result the pollution category S<sub>1</sub> appears to be better related to the observed corrosive environment. This estimation is expected to be confirmed or rejected by the results of the wet candle methodology.

After a comparison of the results of the meteorological and pollution data, and of the gravimetric analysis on carbon steel and aluminum specimens exposed at the coastal site of Pachi, so far, to the expected corrosion damage, estimated by the CDA, there are indications that the CDA does not provide a good correlation between the predicted and the actual corrosion damage at the Pachi Military Airport (Figure 8).

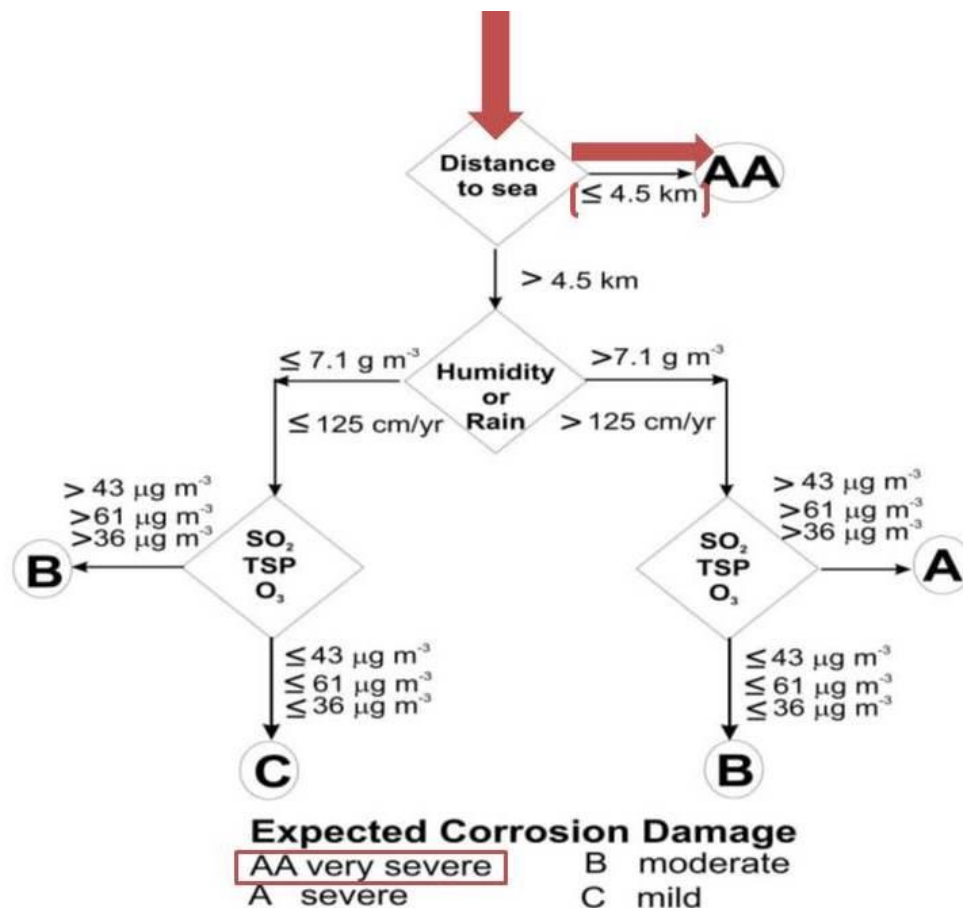


**FIGURE 8.** Section of the Corrosion Damage Algorithm that Considers Distance to Salt Water, Leading Either to the Very Severe AA Rating or a Consideration of the Moisture and the Pollutants and the Expected Corrosion Damage to Carbon Steel and Aluminum Components of the Aircrafts at the Airport (Red Path) Site [14, 15]

The comparison of the classification of atmospheric corrosivity, according to the ISO classification system, to the expected corrosion damage by the CDA at the airport is presented at Table 7.

**TABLE 7.** Comparison of the classification of Atmospheric Corrosivity, According to the ISO Classification System, to the Expected Corrosion Damage by the (CDA) at the Pachi Airport.

Pachi airport	Metal	
	Unalloyed Carbon Steel	Commercially Pure Aluminum
ISO Classification of Corrosivity of Atmospheres	C2 “LOW	C2 “LOW
CDA Classification of Corrosivity of Atmospheres	AA “very severe”	

### Characterization of the Metals Surfaces after 2 Years of Exposure

In the case of unalloyed carbon steel traces of sulphur, carbon and chloride, attributed to the aircrafts fuel emissions and the proximity to the sea (0.2 Km) respectively, are detected from the carbon steel specimens surface analysis by Scanning Electron Microscope/Energy Dispersive Spectrometer (SEM/EDS). Indications of hydroxychlorides and sulfides formation are also detected on both sides probably because of the small thickness of the corrosion layers or the water solubility of the corrosion products. Carbon Steel exhibits the highest concentration of oxygen among the tested metals due to the oxides and hydroxides formed. Growth of oxides, hydroxides and hydroxychlorides are observed, both in skyward and downward sides, already out of the 1st semester of exposure by X-ray Diffraction (XRD). Lepidocrocite and traces of goethite were identified after two years of exposure of carbon steel specimens surface in the atmosphere independently from the initial time of exposure (summer or winter) and the side of the specimens (skyward or downward). Magnetite is identified on the specimens’ skyward surface, exposed during winter, after 2 years of exposure. The corrosion products development on steel surface observed by Optical Microscope (OM) and by X-ray Diffraction (XRD), during the 2-year exposure period, for both initial time of exposure, is presented at the Figures 9 and 10 below.



**FIGURE 9.** Corrosion products developments on steel surface observed by OM.

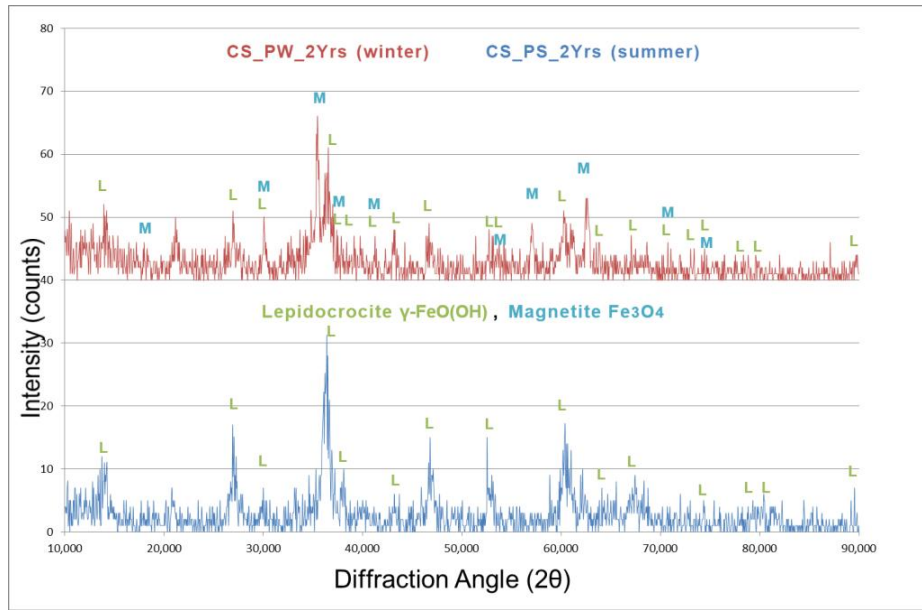


**FIGURE 10.** Corrosion Products Developments on Steel Surface (Skyward Side) Identified by X-ray Diffraction (XRD) After a 2-Year Exposure Period.

The corrosion products development on the copper surface observed by Optical Microscope (OM), during the 2-year exposure period, is presented at Figure 11.

		Before the exposure	After 1 Year of Outdoor Corrosion		After 2 Years of Outdoor Corrosion	
			Summer	Winter	Summer	Winter
Skyward side						
Downward side						

**FIGURE 11.** Corrosion products developments on copper surface

In the case of copper, increased concentrations of oxygen and chlorides are detected by SEM/EDS. Copper exhibits the highest concentration of chlorides among the tested metals. On the skyward side of copper specimens (x100), after 2 Years of exposure (exp. start: Winter and Summer) the % atomic concentration of oxygen, sulphur and chloride were 57% O, 0.5% S and 6-9% Cl, respectively. On the zoomed in area of the Back Scattered Electron image of copper specimen by SEM/EDS (area on the frame of Figure 12), after 2 years of exposure, the % atomic concentration of oxygen, sulphur and chloride detected by SEM/EDS was 61.5% O, 0.5% S and 8.35% Cl respectively).

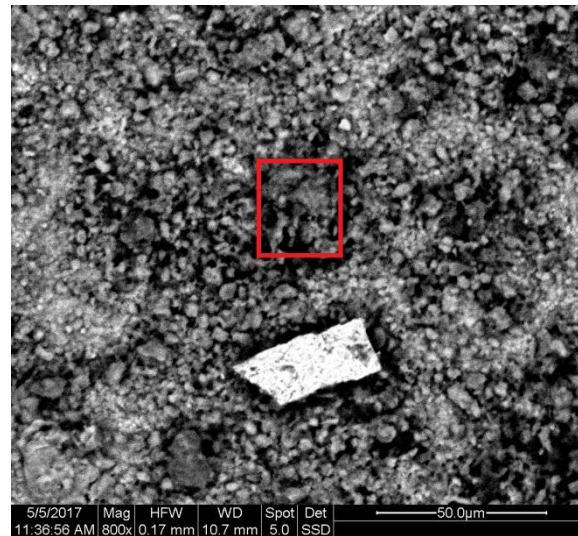


**FIGURE 12.** Back Scattered Electron Image (BSE) of Copper Specimen (Skyward Side) x800, After 2 Years of Exposure (Exp. Start: Winter), with detected local chloride attack

Growth of oxides and hydroxides both in skyward and downward sides, already out of the 1st semester of exposure, has been observed by XRD. Cuprite ( $\text{Cu}_2\text{O}$ ) is identified as the main corrosion product, at both sides of the specimens, after the 2-year outdoor exposure.

In the case of zinc, no visual significant corrosion impact is observed. Local traces of sulphur, due to aircrafts fuel emissions, are observed. No chloride compounds are detected. The high TOW favors the dissolution of zinc chlorides in moisture film. On the skyward side of zinc specimens (x800), after 2 Years of exposure (exp. start: Winter and Summer) the % atomic concentration of sulphur and oxygen were 0.49% S and 34.9% O respectively.

In the case of aluminum, no visual significant corrosion impact is observed. Oxygen, traces of sulphur & chlorides are only locally detected by SEM, after a 2-year exposure period, despite the aircrafts fuel emissions, the proximity to the sea, and the aluminum susceptibility to pitting corrosion. Pitting is macroscopically and microscopically detected on aluminum specimens surface, but in a much smaller extent than theoretically expected and only after 2 years of exposure, due to (i) the pollution of the area ( $\text{SO}_2$  and salinity), (ii) the existing PMs in the area (augmented seasonally by the North African dust), (iii) the meteorology of the area during summer (low RH-TOW and precipitation) and (iv) the presence of the aircrafts in the area. During the transition spring and autumn periods the impact of African dust reaches its peak and increases the particulate matters ( $\text{PM}_{10}$ ) concentrations in the Greek region [74]. It was also observed that the driest months, with lowest rainfall and RH, are July and August [40]. The continuous take-offs/landings and technical tests, during summer, provoke the maximization of the deposition of sulphur dioxide locally, the continuous resuspension and dry re-deposition of the contaminated with sulphur dioxide particulate matters (PMs), on their peak concentration, that guide to relative higher pitting, in density and depth, to the aluminum exposed during summer, as it is presented at Table 8. The surface morphology development of the skyward side of the Aluminum 1050 by AFM, after two years of exposure is presented in Figure 13.

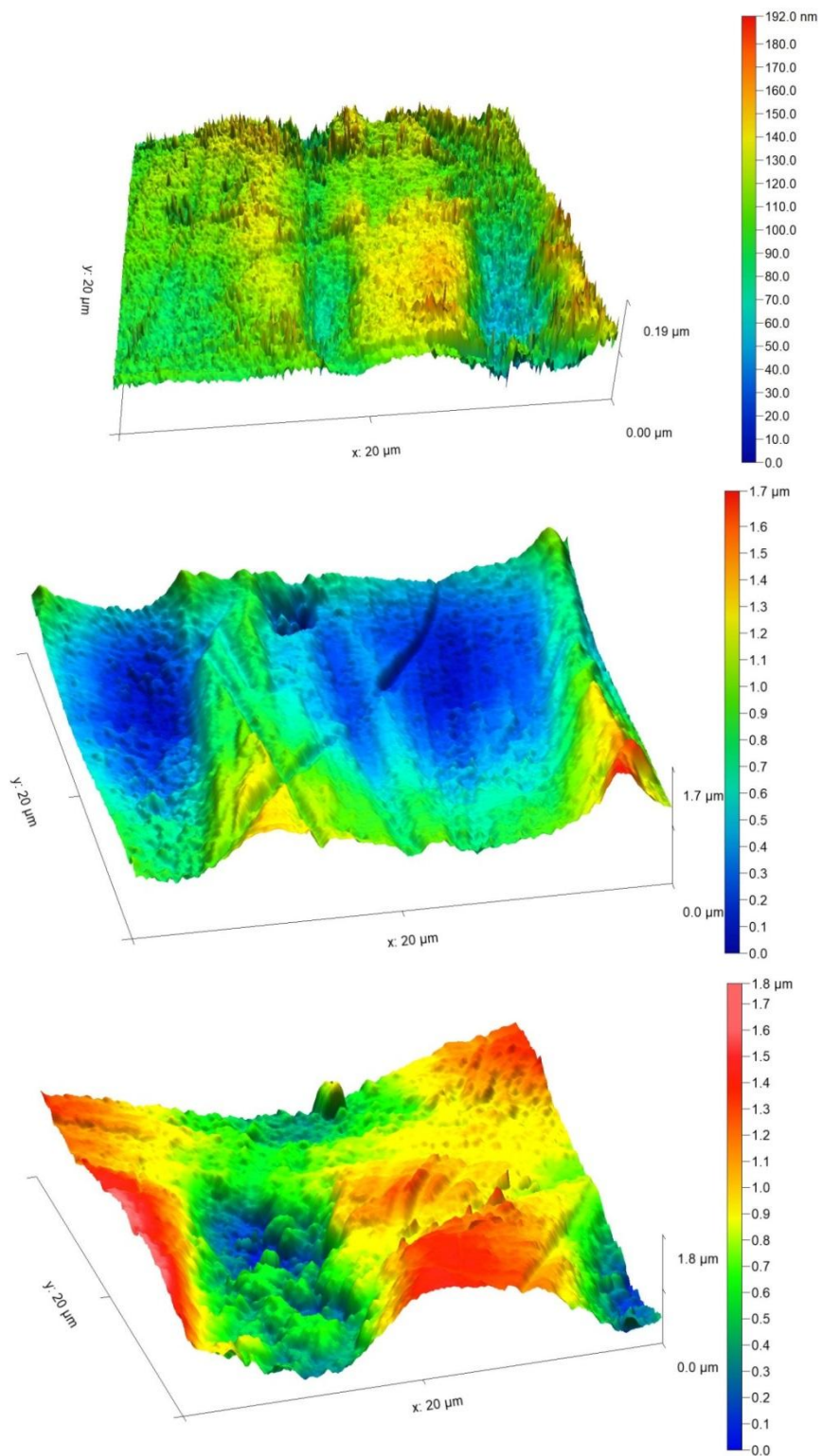


**FIGURE 13.** Surface morphology of the skyward side of the Aluminum 1050 by AFM, before and after 2 years of exposure during summer and winter respectively

The mean roughness ( $S_a$ ) of the  $400 \mu\text{m}^2$  projected areas of the skyward side of the aluminum 1050, before and after 2 years of exposure during summer and winter, was: 65.2, 131 and 136 nm, respectively. After two years of exposure the mean roughness doubles and the grinding lines appear to be filled with corrosion products. No seasonal deviations are observed regarding the roughness evolution of the aluminum surface at Pachi airport. The rating system for the evaluation of pitting corrosion on aluminum was performed in accordance with ISO 8993[75], after 2 years of exposure. The ISO rating has been done visually and the estimation of the average pitting depth in  $\mu\text{m}$  by OM.

**TABLE 8.** Depth of Pits Observed on the Surface of the Aluminum Samples and Evaluation of Pitting Corrosion on Aluminum by OM in accordance with ISO 8993:1989 [75]

Exposure Start	Average Pitting Depth in $\mu\text{m}$	Rating	Percentage of Area of Defects
Summer (S)	2	E6	>0.07 and <0.100
Winter (W)	1.5	E1	

A synopsis of the corrosion products formed on metal surfaces, at both sides, and identified by X-ray Diffraction (XRD) is presented at Table 9.

**TABLE 9.** Corrosion products formed on metal surfaces, after a 2-year exposure period

Metal	Pachi/Summer	Pachi/Winter	Observations	
Aluminum	-	-	No products, at both sides of the specimens, are identified by X-ray diffraction analysis due to the small thickness of the corrosion layers.	
Carbon Steel	Skyward	Lepidocrocite $\gamma\text{-FeO(OH)}$	Lepidocrocite $\gamma\text{-FeO(OH)}$ Magnetite $\text{Fe}_3\text{O}_4$	Traces of goethite identified after 2 years of exposure. Formation of hydroxide chlorides and sulfides were not identified probably because of the small thickness of the corrosion layers or the water solubility of the corrosion products.
	Downward	Lepidocrocite $\gamma\text{-FeO(OH)}$		
Zinc	-	-	No products, at both sides of the specimens, are identified by X-ray diffraction analysis due to the small thickness of the corrosion layers.	
Copper		Cuprite $\text{Cu}_2\text{O}$	Cuprite ( $\text{Cu}_2\text{O}$ ) is identified as the main corrosion product, at both sides of the specimens, after 2-year outdoor exposure.	

Due to the combustion of fossil fuels at the airports region, an atomic concentration of 15-25% of carbon is detected to all metal specimens surfaces by SEM, after 2 years of exposure.

## CONCLUSIONS

- Pachi military airport atmosphere is classified on TOW as T3, according to the ISO9223. Relative Humidity is identified as the major factor of corrosion of metals in the airport. Depending on the metal, the RH in conjunction with:
  - (i) the high PMs concentration, especially during autumn, increases aluminum pitting depth and density and leads to higher corrosion rate of the aluminum exposed during summer,
  - (ii) the airborne salinity and the high concentration of O<sub>3</sub> pollutant leads to relative high corrosion rate of copper,
  - (iii) the effect of sulphur-containing substances and of salinity leads to higher corrosion rate of steel and
  - (iv) the effect of sulphur-containing substances leads to a higher corrosion rate of zinc.
- Regarding the existence of SO<sub>2</sub> pollutant, the area has been classified in pollution category P<sub>0</sub>, which is considered to be background pollution by sulphur dioxide and insignificant from the point of view of corrosion attack.
- According to the experimental findings the chloride deposition rate on carbon steel and aluminum specimens is expected to be between the values 3<S<60, in mg/m<sup>2</sup>d.
- After a comparison of the results of gravimetric analysis on carbon steel and aluminum specimens exposed at the coastal site of Pachi, so far, to the expected corrosion damage estimated by the CDA, there are indications that the CDA does not provide a good correlation between the predicted and the actual corrosion damage at the Pachi Military Airport.
- The ISO classification methodology provides a good correlation among corrosivity of atmospheres and actual carbon steel and aluminum corrosion damage in the specific atmosphere. The atmospheric corrosivity regarding carbon steel and aluminum has been classified as C<sub>2</sub> «Low». These results could contribute to the optimization of the local maintenance management.
- The effects on the metal surfaces from the first-year weight losses underline the necessity of field studies when possible, since the corrosion rate proved to be less than originally expected for all the tested metals, due to the regional topography and the environmental characteristics.
- The 2-year weight loss curves and the 4-year corrosion estimation, show that: carbon steel, zinc and aluminum specimens exposed during winter show significantly higher corrosion rates than those exposed during summer. Zinc in particular, exhibits a corrosion rate one order of magnitude lower than steel. No seasonal deviations are observed regarding the corrosion rates of copper specimens, during the 2-year exposure. The corrosion rates at the coastal site of Pachi are relatively low and are ranked in order of decline: carbon steel>copper>zinc> aluminum.

## ACKNOWLEDGEMENTS

Authors express their gratitude to Hellenic Army/Technical Corps Directorate - Depots Administration - 301 & 307 Depot Commanders **and especially to Major General (Ret.) Mr. Misail Papadakis** for their support. We would also like to acknowledge the valuable assistance provided by 301 Depot's personnel: G. Somos, D. Kontis, N. Tempelis, by the PhD Candidates of the Laboratory of Physical Chemistry of NTUA: O. Papadopoulou and M. Delagrammatikas and by the mechanical engineers Evangelos Brembos and Konstantinos Mylonas.

## REFERENCES

1. H. Simillion, O. Dolgikh, H. Terryn and J. Deconinck, *Corrosion Reviews* (2014).
2. G. H. Koch, M.P.H Brongers, N.G. Thompson, Y.P. Virmani and J.H. Payer, *Corrosion Cost and Preventive Strategies in the United States*. trid.trb.org, 2002.
3. M. V. Biezma and J.R. San Cristobal, “Methodology to Study Cost of Corrosion”, Maney Publishing, 2013.
4. N.G. Thompson, M. Yunovich and D. Dunmire, *Corrosion Reviews*, 25 (3-4) (2007).
5. N.X. Xu, L.Y. Zhao, C.H. Ding, C.D. Zhang, R.S. Li, and Q.D. Zhong, *Corrosion Science*, 44(1), 163-170 (2002).
6. EN ISO 9223:1992. Corrosion of metals and alloys: Corrosivity of atmospheres: Classification, determination and estimation.
7. EN ISO 9224:1992. Corrosion of metals and alloys: Corrosivity of atmospheres: Guiding values for the corrosivity categories.
8. EN ISO 9225:1992: Corrosion of metals and alloys: Corrosivity of atmospheres; Measurement of Pollution.
9. EN ISO 9226:1992. Corrosion of metals and alloys: Corrosivity of atmospheres: Methods of determination of corrosion rates of standard specimens for the evaluation of corrosivity.
10. M. Morcillo, E. Almeida, B. Chico and D. de la Fuente, *Analysis of ISO Standard 9223 (Classification of Corrosivity of Atmospheres) in the Light of Information Obtained in the Ibero-American Micat Project; Outdoor Atmospheric Corrosion*, ASTM 1421, H. E. Townsend, Ed., Ed., American Society for Testing and Materials International, West Conshohocken, PA, 2002.
11. J. Tidblad, *Atmospheric Environment* 55 1-6 (2012).
12. Pourbaix, *Atmospheric corrosion*, John Wiley & Sons, 107 – 121, 1982.
13. McCuen et al. *ASTM STP 1137* 46-76 (1992).
14. S.R. Summitt, F.T. Fink, *Pacer Lime: An Environmental Corrosion Severity Classification System (AFWAL-TLER-80-4102 Part I)*, Metallurgy, Mechanics, and Materials Science, Michigan State University, 1980.
15. NATO Research and Technology Organization, *Corrosion Fatigue and Environmentally Assisted Cracking in Aging Military Vehicles (AG-AVT-140)*, 2011.
16. E.D. Kenny, E.J. Esmanhoto, *Tratamento estatvstico do desempenho de materiais metalicos no estado do Parana*, in: XVII Congresso Brasileiro de Corrosão, Rio de Janeiro, Anais, ABRACO, T-24, 297-308, 1993.
17. E.D. Kenny and E.J. Esmanhoto, *Corrosão do aço-carbono por intemperismo natural no Estado do Parana*, in: IV Seminário de Materiais no Setor Elétrico, Curitiba, Anais, Copel/UFPR, 1994, pp. 377–382.
18. S. Feliu, M. Morcillo and S. Jr. Feliu, *Corrosion Science* 34 403-414 (1993).
19. S. Feliu, M. Morcillo and S. Jr. Feliu, *Corrosion Science* 34 415-422 (1993).
20. L. Mariaca, M. Morcillo, *Funciones de dapo (dosis/respuesta) de la corrosion atmosferica en Iberoamerica: Programa CYTED. Seccion B-7, Gráficas Salu, Madrid, 629-660, 1998.*
21. J. Cai, R.A. Cottis and S.B. Lyon. *Corrosion Science* 41 2001-2030 (1999).
22. Z. Jančíková, O. Zimný and P. Košťal, *Metabk* 52(3) 379-381 (2013).
23. Y. Caia, Y. Zhaob, X. Maa, K. Zhouc and Y. Chenc, *Corrosion Science* 137 163-175 (2018).
24. A. A. Mikhailov, J. Tidblad, and V. Kucera, *Protection of Metals*, 40(6) 541-550 (2004).
25. University of the Aegean, Department of Environment [http://www1.aegean.gr/lid/internet/elliniki\\_ekdosi/TEL\\_DIMOSI/Paper\\_Periferiakotita.pdf](http://www1.aegean.gr/lid/internet/elliniki_ekdosi/TEL_DIMOSI/Paper_Periferiakotita.pdf)
26. Coastline lengths, <http://world.bymap.org/Coastlines.html>.

27. EN ASTM International. Designation:G140-02. Standard Test Method for Determining Atmospheric Chloride Deposition Rate by Wet Candle Method.
28. EN ISO 8407:1991. Corrosion of metals and alloys: Corrosivity of atmospheres: Removal of Corrosion Products from Corrosion Test Specimens.
29. EN ASTM International. Designation G1-90:1999. Standard Practice for Preparing, Cleaning, and Evaluating Corrosion Test Specimens.
30. EN ISO 4221:1980. Air quality Determination of mass concentration of sulphur dioxide in ambient air; Thorin spectrophotometric method.
31. EN ASTM International. Designation: G4458-94 (Reapproved 1999). Standard Test Method for Chloride Ions in Brackish Water, Seawater and Brines.
32. R.D. Klassen and P.R. Roberge, "The Effects of Wind on Local Atmospheric Corrosivity," Corrosion 2001, NACE International, Houston, 2001, Paper # 544.
33. Dean SW, Reiser DB. Analysis of data from ISO CORRAG Program. Corrosion 1998, Paper #340. Houston, TX: NACE International, 1998.
34. S.W. Dean and D.B. Reiser, Comparison of the atmospheric corrosion rates of wires and flat panels. Corrosion 2000, Paper #455. Houston, TX: NACE International, 2000.
35. S.W. Dean, Classifying atmospheric corrosivity - a challenge for ISO. Mater Perform 32(10) 53-58 (1993).
36. P.R. Roberge, R.D. Klassen and P.W. Haberecht, Mater. Design, 23 321–330 (2002).
37. S.W. Dean, Corrosion testing of metals under natural atmospheric conditions. In: Baboian R, Dean SW, editors. Corrosion testing and evaluation: silver anniversary volume. Philadelphia, PA: ASTM, 1990:163176.
38. D. Knotkova and F.N. Speller, Corrosion, 61 723-738, (2005).
39. C. Leygraf and T.E. Graedel, Atmospheric Corrosion, New York, NY, USA, John Wiley and Sons, 2000.
40. C. Titakis, "Quantitative chemical composition of Pachi airport atmosphere and effect of pollutants in aeronautical materials", Diploma thesis, National Technical University of Athens, Greece, 2013.
41. B.E. Psiloglou; Meteorological Data 2009-11, National Observatory of Athens, Institute for Environmental Research and Sustainable Development.
42. Climatology of Elefsina, [http://www.hnms.gr/hnms/english/climatology/climatology\\_region\\_diagrams\\_html?dr\\_city=Elefsina](http://www.hnms.gr/hnms/english/climatology/climatology_region_diagrams_html?dr_city=Elefsina)
43. Hellenic Meteorological Service, [http://www.emy.gr/hnms/english/index\\_html?](http://www.emy.gr/hnms/english/index_html?)
44. H.D. Kambezidis and G. Kalliampakos, Water Air Soil Pollution 224 1463 (2013).
45. Ministry of Environment and Energy, Air Quality Department, Annual Report of Air Pollution, 2016: <http://www.ypeka.gr/LinkClick.aspx?fileticket=81Y3zyY9w%2BU%3D&tabid=490&language=el-GR> (greek).
46. European Environmental Agency/ Sulphur Dioxide (SO<sub>2</sub>): annual mean concentrations in Europe; site: <http://www.eea.europa.eu/themes/air/interactive/so2>.
47. EMEP MSC-W modeled air concentrations and depositions, [http://webdab.emep.int/cgi-bin/webd2\\_controller.pl?State=ydata&reportflag=2015&countries=GR&years=2013&pollutants=total+ox.+sulphur&datatype=grid50\\_png](http://webdab.emep.int/cgi-bin/webd2_controller.pl?State=ydata&reportflag=2015&countries=GR&years=2013&pollutants=total+ox.+sulphur&datatype=grid50_png).
48. EMEP MSC-W modeled air concentrations and depositions, [http://webdab.emep.int/cgi-bin/webd2\\_controller.pl?State=ydata&reportflag=2015&countries=GR&years=2009&pollutants=SO2&datatype=grid50\\_png](http://webdab.emep.int/cgi-bin/webd2_controller.pl?State=ydata&reportflag=2015&countries=GR&years=2009&pollutants=SO2&datatype=grid50_png).
49. P.D. Kalabokas G. Sideris, M.N. Christolis and N.C. Markatos N.C., Analysis of Air Quality Measurements in Volos, Greece; Presented at the 5<sup>th</sup> International Exposition and Conference for Environmental Technology, HELECO, 2005.

50. EMEP MSC-W modeled air concentrations and depositions, [http://webdab.emep.int/cgi-bin/webd2\\_controller.pl?State=ydata&reportflag=2015&countries=GR&years=2013&pollutants=O3&datatype=grid50\\_png](http://webdab.emep.int/cgi-bin/webd2_controller.pl?State=ydata&reportflag=2015&countries=GR&years=2013&pollutants=O3&datatype=grid50_png).
51. A-N Riga-Karandinos and C. Saitanis, *Chemosphere* 59 1125-1136 (2005).
52. U. Ima, S. Christodoulaki, K. Violaki, P. Zampas, M. Kocak, N. Daskalakis, N. Mihalopoulos and M. Kanakidou, *Atmospheric Environment* 81 6 (2013).
53. V.G. Mossotti and A.R. Eldeeb, MORPH-2, a software package for the analysis of scanning electron micrograph (binary formatted) images for the assessment of the fractal dimension of exposed stone surfaces. U.S. Geological Survey, 2000.
54. H. Xiao, W. Ye, X. Song, Y. Ma and Y. Li, *Materials* 10 1262 (2017).
55. M. Pourbaix, "The linear bilogarithmic law for atmospheric corrosion". In *Atmospheric Corrosion*; Ailor, W.H., Ed.; The Electrochemical Society, John Wiley and Sons: New York, USA, 1982; pp.107–121.
56. EN ASTM G16-95, Standard guide for applying statistics to analysis of corrosion data, ASTM, Philadelphia, PA, USA 1999.
57. EN ASTM G 101-01, Standard guide for estimating the atmospheric corrosion resistance of low alloy steels, ASTM, Philadelphia, PA, USA 2001.
58. J. W. Spence, F. H. Haynie, F. W. Lipfert, S. D. Cramer, L. G. McDonald, *Atmospheric Corrosion Model for Galvanized Steel Structures*, CORROSION. 1992;48(12):1009-1019.
59. J. Kobus, *Mater. Corrosion* 51 104 (2000).
60. S. A. Abdul-Wahab, *Toxic Radioactive Waste Management* 7 190 (2003).
61. S. Bhattacharjee, N. Roy, A. K. Dey and M.K. Banerjee, *Corrosion Science* 34 573 (1993).
62. J. J. Santana Rodriguez, F. Javier Santana Hernandez and J. E. Gonzalez, *Corrosion Science* 45 799 (2003).
63. S.W. Dean and D.B. Reiser, *Analysis of Long-Term Atmospheric Corrosion Results from ISO CORRAG Program*, *Outdoor Atmospheric Corrosion*, STP 1421, H.E. Townsend, Ed., American Society for Testing and Materials, 2002, p 3–18
64. H. E. Townsend, *Corrosion* 57(6), 497-501 (2001).
65. M. Morcillo, B. Chico, D. de la Fuente, and J. Simancas, *Int. J. Corrosion* 12 (2012).
66. R. Ericsson, *Werkstoffe und Korrosion*, 29(6), 400–403, (1978).
67. S. Oesch, *Corrosion Science* 38, 1357 (1996).
68. S.C. Chung, A.S. Lin, J.R. Chang, H.C. Shih, *Corrosion Science* 42, 1599-1610 (2000).
69. J.E. Svensson, L.G. Johansson, *J. Electrochem. Soc.* 140, 2210 (1993).
70. X. Odnevall and C. Leygraf, *Corros. Sci.* 36, 1551 (1994).
71. K.A. van Geteren, *Galvanotechnik* 72, 35 (1981).
72. E. Johansson and J. Gullman, *KI Rapport 7*, Swedish Corrosion Institute, 1991.
73. C. J. Slunder and W. K. Boyd, *Zinc: Its Corrosion Resistance*, ILZRO, New York, NY, USA, 1983.
74. C. Mitsakou, G. Kallos, N. Papantoniou, C. Spyrou, S. Solomos, M. Astitha, and C. Housiadas. Saharan dust levels in Greece and received inhalation doses. *Atmos. Chem. Phys.*, 8, 7181-7192, 2008.
75. EN ISO 8993:1989. Anodized aluminium and aluminium alloys - rating system for the evaluation of pitting corrosion – Chart method.